Metabolic Flux Interval Analysis of CHO Cells

F. Zamorano[1], A. Vande Wouwer[1], AL. Hantson[2], G. Bastin[3]

[1]Service d'Automatique, Faculté Polytechnique de Mons, Mons, Belgium;

[2]Service de Chimie et Biochimie appliquées, Faculté Polytechnique de Mons, Mons, Belgium;

[3]CESAME, Université Catholique de Louvain, Louvain-La-Neuve, Belgium

Corresponding author: F. Zamorano, Service d'Automatique, Faculté Polytechnique de Mons,
Boulevard Dolez 31, B-7000 Mons, Belgium, `francisca.zamorano@fpms.ac.be`

Abstract. Based on a detailed metabolic network of CHO-320 cells built using available information gathered from published reports, the flux distribution can be evaluated using tools of positive linear algebra (e.g., the algorithm METATOOL devised in [19, 26]). In particular, it is possible to study the influence of the interconnection level of the network as well as the availability of specific measurement information on its flux distribution. As this latter information is usually not sufficient to completely define the metabolic fluxes (i.e., the linear system of equations is underdetermined and infinity of solution exists), it is of interest to compute the range of possible (non-negative) solutions. Interestingly, depending on the available measurements, the intervals obtained for the intracellular fluxes can be quite narrow, especially for the fluxes surrounding the central metabolism. In this study, the construction of the metabolic network and the selection of its structure (depending on the cell life cycle) are discussed with a view to the determination of the flux distribution. In addition, the sensitivity of the solution space to the availability of specific measurements is assessed.

1 Introduction

The examination of metabolic fluxes under different environmental conditions may result in a better understanding of the fundamental metabolism of cells in culture, which is essential for the design of bioreactors, media formulations and control strategies [34].

The determination and study of metabolic fluxes *in vivo* has been termed Metabolic Flux Analysis and occupies a central place in metabolic engineering [28, 29]. Material balancing can be used to provide estimates of major metabolic pathway fluxes when all significant metabolite uptake and production rates are measured [18, 21]. This approach is based on the *a priori* knowledge of a detailed underlying metabolic network and the use of the fundamental assumption that internal metabolites are in quasi-steady state [7, 16, 18, 24, 34].

When applied to complex networks, material balancing may not be sufficient to uniquely determine all fluxes, as the number of unknown fluxes may exceed the number of linear mass balance equations [7, 18]. Either additional experimental flux data or additional theoretical constraints are required to find one unique flux distribution out of the solution space [4]. Depending on the underlying assumptions, the resulting flux distribution could be very different. Any conclusion about the metabolism of the cell, deduced from a particular flux distribution, should be taken with care.

Depending on the metabolic phase under consideration (for instance the growth phase), reactions can be assumed irreversible (even if in another metabolic phase the reactions are indeed occurring in the reverse way) and the corresponding fluxes non-negative, so that tools of non-negative linear algebra, or convex analysis, can be exploited to compute the set of admissible solutions [20]. In particular, METATOOL [19, 26] allows the computation of the non-negative space of solutions, and as an extension intervals for each metabolic flux.

The focus of this study is on metabolic flux analysis of complex networks in the usual situation where extracellular data are not sufficient to provide the missing information required to define a unique solution to the mass balance system. To this end, a detailed metabolic network of CHO cells is first built based on published reports. The validity of the network structure is tested by considering alternative network configurations, i.e., the selection of the flux directions, depending on the cell life cycle. Using METATOOL, intervals bounding the metabolic fluxes are computed in a straightforward way, and the influence of specific measurement information is assessed.

This paper is organized as follows. Section 2 describes how a detailed metabolic network of CHO cells has been built. The set of experimental data is briefly described in section 3. In section 4, the methodology used for the metabolic flux interval analysis is introduced, some numerical results are presented and a few case studies are discussed. Finally, section 5 draws conclusions and perspectives.

2 Metabolic Network Description

For the representation of the metabolism of CHO cells, a metabolic network based on several series of bioreactions of a generic mammalian cell has been built. This graphical representation of the metabolism includes:

- Glycolysis;

- Pentose Phosphate Pathway;

- Tricarboxylic Acid Cycle;

- the Amino Acid metabolism and Protein and Antibody Synthesis;

- the Urea Cycle

- the Nucleic Acid Synthesis;

- the Membrane Lipid Synthesis.
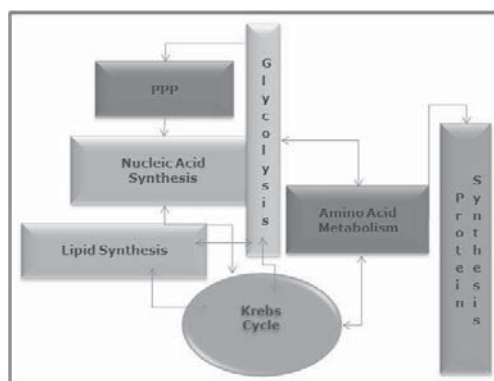
Figure 1: Schematic Representation of the Metabolic Network for CHO-320 cells

Numerous works deal with metabolic flux analysis of animal cells, like Hybridoma [4, 6, 33], HEK-293 [10, 16], MDCK [32] and CHO cells [2, 20, 22]. The metabolic networks described in all these studies consider the main catabolic and anabolic pathways occurring within the cell with a relatively limited level of complexity. Among all these studies the central metabolism considered remains quite similar, with the exception of a few reactions which are specific to each type of mammalian cell.

2.1   Central Metabolism

The Central Metabolism comprises Glycolysis, the Pentose Phosphate Pathway and the Tricarboxylic Acid Cycle. Although metabolism embraces hundreds of different enzyme-catalyzed reactions, the central metabolic pathways (present in all organisms), are limited in number and remarkably similar in all forms of life [17]. Even if it is possible to find slight differences between different cell kinds, they are hardly noticeable among mammalian cells, with the exception of course, of genetically manipulated cell lines. The central metabolism considered herein is the usual metabolism used for strictly aerobic eukaryotic organisms [2, 5, 6, 18, 20, 33].

As intermediates of the TCA cycle are removed to serve as biosynthetic precursors, they are replenished by anaplerotic reactions. Normally, the draw off and the replenish reactions are in dynamic balance, thus concentrations of TCA cycle intermediates remain almost constant. Among the most common anaplerotic reactions, the reversible reaction catalyzed by malic enzyme is widely distributed in eukaryotes and prokaryotes [17].

The main carbon and energy sources for mammalian cells in culture are glucose and glutamine, the latter also serving as the primary nitrogen source. There are additional requirements for other nutrients, but their contribution to energy metabolism is small compared to the demand for the main substrates [34]. Hence, the contribution of amino acids to energy production has often been neglected. Major products of glucose and glutamine metabolism are biomass, secreted protein, energy in de form of ATP, reducing power for biosynthesis, carbon dioxide, and the waste products lactate and ammonia [34].

2.2   Amino Acid, Protein & Antibody Metabolism

Regarding the amino acid metabolism in mammalian cells, essential amino acids, which cannot be synthesized by the cell and must therefore be provided in the culture medium, are only considered in the catabolic phase. In contrast, for non-essential amino acids (produced by the cell metabolism and possibly not supplied in the culture medium), both, anabolic and catabolic phases are taken into account. The pathways of amino acids catabolism are quite similar in most organism. The routes of their degradation converge to the central catabolic pathways, where their carbon skeleton find the way to the TCA cycle, and their amino group is shunted into other routes. The catabolic pathways of all 20 amino acids converge to form only five products, all of which enter the TCA cycle: Acetyl-CoA, Oxaloacetate, Fumarate, Succinyl-CoA and α-ketoglutarate [17]. All catabolic reactions of amino acids and biosynthetic reactions of nonessential amino acids have been taken from references [1] and [17] based on metabolic pathways of several mammalian organism.

The cell line CHO-320 was derived from a mutant of the CHO-K1 cell, transfected with human IFN-γ to synthesize and secrete this antibody [14, 20]. This cell line is auxotrophic with respect to proline, and thus it cannot synthesize proline from either ornithine or glutamate and relies on its external supply for growth [13]. Hence, Proline for CHO cells is also an essential amino acid among the classical ones (His, Ile, Leu, Lys, Met, Phe, Thr, Trp, Val).

Mammalian tissue is ureotelic, which means that the excess NH_3 is converted into urea and then excreted [4]. Accordingly, small amounts of urea can be detected during CHO-320 cell cultures. Hence, the Urea Cycle has been included as a part of the metabolic network of CHO-320 cells.

Since proteins are built to play a specific role, and sometimes, their composition and structure depend on the organisms that produce them, their composition and dimensions can vary widely. Therefore, it is not possible to establish a standard protein composition, given that the stoichiometric coefficients should be evaluated for each organism and each type of protein. In [20] an average composition of proteins for eukaryotic cells is presented, composition that does not differs from the percentage of amino acids occurrence in proteins given in [17]. Thus, an average stoichiometric pattern based on these references has been considered to simulate protein synthesis as a simplified reaction. In the same way, the reaction synthesis of the INF-γ antibody is a simplified reaction whose stoichiometric pattern is based on its known amino acid sequence [8, 9, 15]. In table 1 the different contributions of amino acids to protein and INF-γ synthesis are presented.

Table 1: Average Stoichiometric Composition for Protein and INF-γ Antibody Synthesis

Amino acids	Percentage of occurrence in Proteins	Percentage of occurrence in INF-γ
Alanine	7.8	5.48
Arginine	5.1	5.48
Histidine	2.3	1.37
Asparagine	4.3	6.85
Cysteine	1.9	1.37
Isoleucine	5.3	4.79
Aspartate	5.3	6.85
Glutamine	4.2	6.16
Leucine	9.1	6.85
Glutamate	6.3	6.16
Glycine	7.2	3.42
Lysine	5.9	13.7
Serine	6.8	7.53
Proline	5.2	1.37
Methionine	2.3	2.74
Tyrosine	3.2	3.42
Phenylalanine	3.9	6.85
Threonine	5.9	3.42
Tryptophan	1.4	0.68
Valine	6.6	5.48

2.3 Nucleotide Metabolism

Nucleotide synthesis, and in turn *DNA* and *RNA* synthesis, only considers the *de novo* pathways, i.e., they are synthesized from its main precursor: *Ribose*5 − *Phosphate*, final product of the Pentose Phosphate Pathway. The second route leading to nucleotides, *the salvage pathway*, is not considered herein because it recycles the free monomers released from nucleic acid breakdown. As this study does not consider degradation of nucleic acids, the salvage pathways of synthesis are not considered into the metabolic network. The *de novo* pathways for purine and pyrimidine biosynthesis appear to be identical in nearly all living organism [17].

DNA and *RNA* structures are slightly different. Both molecules contain two major purine bases, adenine and guanine, and two major pyrimidines. Cytosine is one of the pyrimidines in both nucleic acids, but the second is thymine in *DNA* and uracil in *RNA* [17]. In order to simulate nucleic acids synthesis as two simplified reactions (in a similar way as for proteins), average percentages of nucleotide composition have been considered. In [27, 30, 31] an average composition of nucleic acids is given, at different Guanine-Cytosine base concentrations for several cell types. On this base, two overall reactions for both *RNA* and *DNA*, can be established.

2.4 Lipid Metabolism

Among all different kinds of lipids, we only consider those which play a structural role as components of membranes. There are three general types of membrane lipids: Glycerophospholipids, Sphingolipids and Sterols. The carbon chains of fatty acids (phospholipids major components), are assembled in a repeating four step sequence

which is the same in all organisms [17]. The most common unsaturated and monounsaturated (a single double bond) fatty acids of animal tissues are palmitate (16:0) and stearate (18:0), and palmitoleate (16:1) and oleate (18:1), respectively [4, 17]. Usually, glycerophospholipids contain one saturated fatty acid (C_{16} or C_{18}), and one unsaturated fatty acid (C_{18} to C_{20}) [17]. Hence, the synthesis of phospholipids herein is in agreement with the last statement.

It is assumed that CHO-320 cells are able to synthesize Cholesterol, due to its fundamental role in the structure of many membranes and because in mammalian cells, cholesterol can be synthesized from acetate precursors [17, 23].

In [11, 12, 17] usual percentages of membrane phospholipids are specified. In order to represent an overall reaction for the synthesis of an average membrane lipid, its phospholipid composition has been established on the base of these reference values.

It is worth mentioning that the metabolic network built for this study, corresponds to a metabolism of growing cells. Therefore, a specific flux direction has been assigned to some of the reactions according to this phase of the cell life. The complete series of bioreactions included in the metabolic network studied in the present work, are presented in Appendix A. The analysis of the complete network has been done using the method described hereafter.

3   Experimental data base

The experimental data base originates from CHO-320 cells cultures used in [20, 21]. These experimental data correspond to measurements collected from three different batch cultures of a CHO-320 cell line. This data set contains the extracellular concentrations of the main substrates: Glucose and Glutamine; the main metabolism excretion products: Lactate, Alanine and Ammonia; and the concentration of 14 additional amino acids, along with the evolution of the biomass inside the bioreactor during the growth phase.

4   Metabolic Flux Analysis

4.1   Method

4.1.1   Pseudo steady-state assumption

A high turnover of the pools of most intracellular metabolites is supposed to happen within the cells, and it is therefore reasonable to formulate the assumption of balanced growth paradigm. This hypothesis states that inside growing cells, all internal metabolites are in quasi-steady state, i.e., for each internal metabolite involved in a given metabolic network, the production and consumption fluxes are balanced, and so, the net sum is zero. The quasi-steady state condition is mathematically expressed by a mass balance equation of the internal metabolites with no accumulation (zero time derivatives). This can be expressed by means of the stoichiometric matrix N and the flux distribution vector v.

$$N \cdot v = 0 \tag{1}$$

It is worth noting that v is a non-negative vector, since the flux direction is fixed depending on the particular metabolic phase (growth, maintenance, death) under consideration. This is different from considering irreversible reactions. Loads of the metabolic reactions are reversible, but they have a predominant direction depending on metabolic conditions. Therefore, each of them could be seen as a net reaction with a fixed direction.

The algebraic relation (1) between the intracellular fluxes around the intracellular metabolites is the fundamental equation that underlies the metabolic flux analysis.

4.1.2   Metabolic Flux Analysis

Metabolic Flux Analysis is a methodology in metabolic engineering for the quantification of pathway fluxes when extracellular measurements are the only available data. By building a proper metabolic network for the intracellular reactions and applying steady state mass balances around the internal metabolites, an admissible flux distribution can be found. This solution is represented as a vector, where its entries are the rates at which each reactions take place.

The specific uptake and excretion rates of the measured external species (v_m) are linear combinations of some of the metabolic fluxes, thus, by defining a proper matrix N_m, the specific consumption and production rates can be expressed as:

$$v_m = N_m \cdot v \tag{2}$$

The aim of metabolic flux analysis is to compute the unknown (non-negative) vector v from measurements v_m. Thus, the admissible flux distribution v must now satisfy the complete system (3), in order to agree with the experimental data.

$$\begin{pmatrix} N \\ N_m \end{pmatrix} \cdot v = \begin{pmatrix} 0 \\ v_m \end{pmatrix} \tag{3}$$

In general, this system is underdetermined, as a metabolic network happens to be composed of less nodes (internal metabolites) than connections (reactions), and usually, the number of external measurements is not sufficient to provide the missing information, i.e., the missing linear equations in system (3). Therefore, the solution of the system is not unique but admits a set of admissible non-negative flux distributions.

System (3) constraints the set of solutions, as solutions compatible with observed measurement data are now sought. The constrained solution set, called Flux distribution Space F, is obtained from:

$$\begin{pmatrix} N & 0 \\ N_m & -v_m \end{pmatrix} \cdot \begin{pmatrix} v \\ 1 \end{pmatrix} = 0 \tag{4}$$

The set F of admissible solutions is a convex polyhedral cone whose edges, the extreme rays f_i give any admissible vector v by an appropriate non-negative linear combination.

$$v = \sum_i \alpha_i f_i \text{ with } \sum_i \alpha_i = 1 \text{ and } \alpha_i \geq 0 \tag{5}$$

The extreme rays are obtained by applying the software METATOOL [19] to the first matrix of equation (4).

The flux distribution space F provides the limiting values of the flux interval for each metabolic flux. This is, every extreme ray provides a particular solution to v, and in turn, to every metabolic flux. Thus, among all possible values that v_i may have, there will be an upper and a lower value which will define the limits for this flux v_i. The bounds $v_i^{\min}$ and $v_i^{\max}$ can be defined from the convex basis vectors f_i of the flux space as:

$$v_i^{\min} \underline{\Delta} \min\{f_{ki}, k = 1, ..., p\} \tag{6}$$

$$v_i^{\max} \underline{\Delta} \max\{f_{ki}, k = 1, ..., p\} \tag{7}$$

where f_{ki} represents the $i-th$ element of the basis vector f_k of the flux space F.

4.2 Numerical Results

The metabolic network (N) representing the intracellular mass balances at quasi steady-state, includes 118 bioreactions and 80 internal metabolites. Together with the available measurements in table 2, the system of equations (4) reaches a final dimension of 99×118.

Table 2: Extracellular Measurements in $[mmol/h \cdot 10^9 cell]$

| $v_{glucose}$	$v_{glutamine}$	$v_{lactate}$	$v_{alanine}$	$v_{ammonia}$		
0.1781	0.0502	0.3445	0.0457	0.0088		
v_{arg}	v_{asn}	v_{asp}	v_{glu}	v_{gly}	v_{ser}	v_{thr}
$2.1417e^{-3}$	$1.1278e^{-3}$	$3.1785e^{-3}$	$9.5475e^{-4}$	$2.2295e^{-3}$	$9.2342e^{-4}$	$1.1842e^{-3}$
v_{ile}	v_{leu}	v_{lys}	v_{met}	v_{phe}	v_{tyr}	v_{val}
$1.5278e^{-3}$	$2.6013e^{-3}$	$2.1245e^{-3}$	$7.2375e^{-4}$	$9.9808e^{-4}$	$7.6104e^{-4}$	$1.9561e^{-3}$

With the above described set of measurements and the previously defined metabolic network, the admissible space of solutions is computed with METATOOL from system (4). In this case, the constraints imposed by the external measurements are not strong enough to provide a well restricted range of fluxes. Although, a limited set of flux distributions is found (see Fig. 2), some important inputs are missing (as His, Cys, Pro and Trp), which generates a large uncertainty on their uptake (or eventually production) rates. These non-measured uptake or production rates may vary significantly within their (mathematically) admissible ranges and as a consequence, the metabolic fluxes of the reactions which are directly or indirectly connected to them can undergo large variations. Thus, in order to be able to limit the flux ranges, it is required to possess additional measurement information.

4.3 Case studies

4.3.1 Testing different network structures

As already pointed out, the metabolism involves several reversible reactions, whose net direction is not *a priori* known and depends on the metabolic phase of the cell (i.e., if a reversible reaction operates in both directions, then a net positive flux should occur in the designated direction). In the metabolic network under consideration, a fixed flux direction is given to each biochemical reaction according to the corresponding metabolic phase. Nevertheless, there are some reversible reactions whose net direction cannot be decided only on the basis of the metabolic phase of the cells. It is the case of the reactions in figure 3, which can run in both directions depending on the need for some metabolites in particular reactions or pathways. To calculate the solution space presented in the previous subsection, a particular choice has been made for the direction of these four reversible reactions (as they appear in Appendix A). Nevertheless, as other configurations might be possible, it is useful to test them, i.e., to change
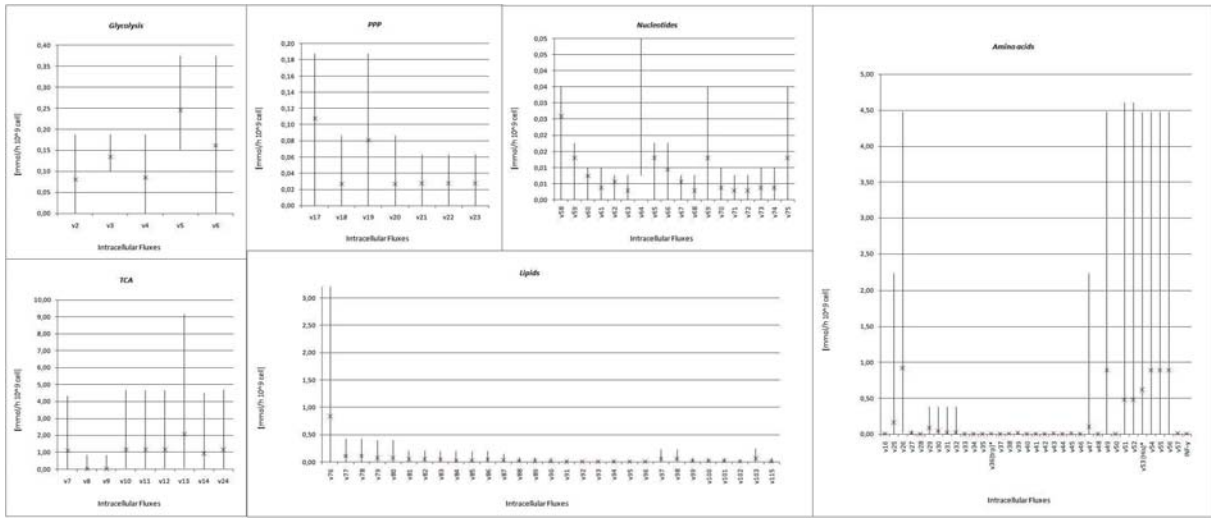
Figure 2: Flux Distribution Intervals. Red crosses indicate the mean value of each flux, which is also a particular solution. (*) v_{64} upper limit reaches $4,4707$ $[mmol/h \cdot 10^9]$.
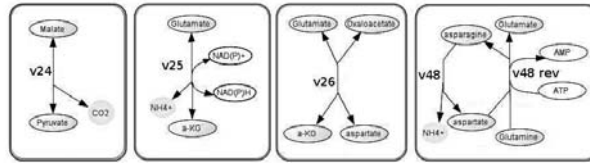
Figure 3: Reversible Reactions

the direction of these reactions and to investigate if a solution to the flux analysis exists. Among the 16 possible flux distributions that can be obtained by changing the direction of the above reactions, only two of them possess a solution space, i.e., only two network configurations admit a solution satisfying the constraints imposed by the extracellular measurements (experimental data of table 2). One of them is obviously the configuration considered to calculate the solution space of the previous subsection. The second admissible configuration is characterized by:

$$v_{24} : Malate \rightarrow Pyruvate + CO_2$$
$$v_{25rev} : \alpha KG + NH_4^+ + NAD(P)H \rightarrow Glu + H_2 0 + NAD(P)^+$$
$$v_{26} : Oxaloacetate + Glu \rightarrow Asp + \alpha KG$$
$$v_{48} : Asn \rightarrow Asp + NH_4^+$$
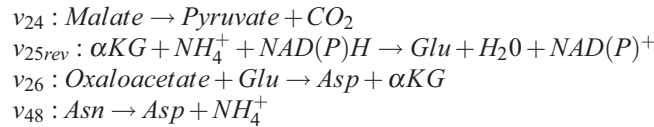
This latter flux distribution implies the occurrence of reaction v_{25} in the reverse direction, from α-ketoglutarate to glutamate, which has generally been reported to be feasible in cultures under high ammonia concentrations. Normally, this reaction produces α-ketoglutarate from glutamate, as a second step of the metabolic pathways for glutamine degradation [25]. Also in other kind of mammalian cells, specifically Hybridoma cells cultures, it has been demonstrated that under ammonia-stress conditions, the reaction catalyzed by glutamate dehydrogenase (reaction v_{25}) goes in the reverse sense, while control cells transform glutamate in α-ketoglutarate and ammonia [5]. In our CHO cell culture, ammonia is constantly produced and accumulated, but its concentration during the growth phase is probably not sufficient to stimulate the shift of direction in v_{25}, even if it is mathematically possible. In [5] the ammonia-stress condition is given by 10 mM of ammonia, while, in our culture at the end of the growth phase its concentration only reaches 5 mM.

This kind of test can also be achieved for the extracellular measurements, i.e. to check that if a metabolite is assumed being consumed whereas it is normally produced (or vice versa), no valid flux distribution intervals can be found. Considering the reaction sequences in the correct direction allows a feasible flux distribution to be obtained. To our eyes, this can be interpreted as a sign of the consistency of our metabolic network.

4.3.2 Measurements Sensitivity

Depending on the number and type of available extracellular measurements, the number of basis vectors f_i changes, as well as the size of the flux intervals. Some measurement information appears as critical for the determination of the flux intervals, whereas some other measurement inputs are less influencial. In order to determine which

measurements are required to compute relatively narrow flux intervals, we test the effect of the presence/absence of particular extracellular measurements on the solution space.

Generally, one can rely on glucose, lactate and ammonia measurements, as their quantification procedures are quite simple and widespread. On the other hand, the determination of all amino acid uptake and excretion rates can be more delicate and time-consuming. Thus, in the following, we focus attention on the impact of the availability of measurement information for the amino acids uptake and excretion rates. As in our experimental data base, the measurements of four of the amino acids are not available, an estimation is first achieved based on the literature [3] so as to "virtually" complete the data base.

To proceed with the analysis, one of the twenty (16 real and 4 estimated) amino acid measurements is removed (one at the time), in order to see in which way this particular measurement affects the obtained flux intervals. As a result, two groups of amino acid measurements are found. The first one includes measurements whose absence increases the size of the intervals of up to 100%. These amino acids, listed from lower to higher impact, are: Gly, Ala, Trp, Met, Cys, Thr, Ser and Asp. The second group includes measurements whose availability has a much larger influence on the interval size. Again from lower to higher impact, the corresponding amino acids are: Lys, Leu, Tyr, Phe, Ile, Val, Pro, Glu, Asn, His, Gln and Arg. In order to ilustrate the range in which the intervals are varying, the highest percentages of increase (for each metabolic routes) are presented in table 3.

Table 3: Increase of flux intervals in relation with amino acid measurements

Metabolic Pathway	First Group of Amino acids (%)	Second group of Amino acids (%)
Glycolysis	50.7	239.9
TCA	86.0	4867.0
PPP	17.2	116.0
Urea Cycle	96.6	9697.4
Nucleotides	118.9	11927.4
Lipids	62.7	3107.9

Apparently, the variation in the flux interval sizes significantly depends on which amino acid (uptake or production) measurement is missing and on the degree of interconnection of the internal routes that follow (or precede) each consumption (or production) reaction. In addition, we have tested different scenarios where several amino acid measurements of the first group are missing, and it has been found that three, four or even five of these measurements can be missing, while obtaining still reasonable percentages of increase in the interval sizes (table 4).

Table 4: Percentage of increase of the interval size generated by missing measurements of the First group

Pathway	Gly, Ala, Met	Gly, Ala, Cys	Gly, Ala, Ser	Gly, Ala, Asp	Gly, Ala, Met, Cys	Gly, Ala, Met, Asp	Gly, Ala, Met, Cys, Ser
Glycolysis	25.7	38.4	40.0	57.5	38.5	62.0	40.0
TCA	48.2	89.8	89.5	102.8	90.2	286.0	97.5
PPP	12.6	17.2	17.2	17.2	17.2	17.2	17.2
Urea Cycle	37.0	91.6	91.6	115.6	91.6	304.2	91.6
Nucleotides	63.7	131.1	130.6	160.1	131.2	392.3	131.2
Lipids	23.6	59.7	64.5	74.3	60.7	193.7	64.5

4.3.3 Hypothetical additional measurements

By estimating the uptake or production rate of a number of species, the metabolic flux intervals can be significantly restricted in their size, thus providing useful estimation of the flux distribution. Starting from the assumption that we possess the measurements of all 20 amino acids and that we are able to measure a few more extracellular (substrates or products) metabolites, we analyze in which order of magnitude these additional constraints reduce the size of the intracellular flux intervals.

Five hypothetical measurements have been considered in this analysis, where three out of them are usually (or easily) measured: urea uptake rate, CO_2 evolution rate (CER) and antibody production rate ($INF - \gamma$). The other two, Choline and Ethanolamine uptake rates, may need more specific methods for their determination, which are however still practicable. As the latter two are the only extracellular inputs of the Lipid Pathways, they should carry valuable information.

The essays are systematically performed including one measurement at a time. The percentages in which the flux intervals are reduced are shown in figure 4. Clearly, each measurement has a different effect over the different metabolic pathways. The knowledge of the urea uptake rate, for example, drastically reduces the intervals of the nucleotide pathways (60%), the urea cycle (97%), and some reactions involved in the metabolism of ammonia. By measuring the CER, the pathways of the central metabolism (Glycolysis, TCA and PPP) are very significantly reduced. On the other hand, the measurement of $INF - \gamma$ production rate only reduces the uncertainty of the amino

acid catabolism fluxes, as amino acids are direct precursors of the antibody. Finally, it seems that the measurement of choline should be enough to effectively reduce the flux intervals of the lipid pathways. Interestingly, it appears that choline is a more informative measurement than ethanolamine. Ethanolamine enters in a small cyclic route involving phosphatidylserine and phosphatidylethanolamine, which may result in a system with more degrees of freedom than the system obtained when choline is measured. The result of this analysis is quite practical, and hence, one would be able to decide which metabolites provide the more usefull information and thus, which are to be measured instead of others. In our case, the more informative measurements appear to be the CER and urea and choline uptake rates. By measuring these extracellular metabolites, the intervals are significantlty reduced. Even if the measurement of the antibody production does not seem to be very informative, it is of fundamental interest to measure it, since $INF - \gamma$ is the main product of interest of CHO-320 cell cultures.

5 Conclusions

In this study, a detailed metabolic network of $CHO - 320$ is built based on information available in the literature. Together with the classical assumption that the internal metabolites are in quasi-steady state, the measurements of the time evolution of a number of culture components provide a set of constraints on the metabolic network. However, the number of measurements is usually not sufficient to fully determine the flux distribution, and it is necessary to resort to the concept of Flux Space, which defines admissible ranges for the flux distribution.

Based on a set of limited available measurements of extracellular components, alternative network configurations, corresponding to different net directions of several reversible pathways, are systematically investigated. Among the 16 candidate configurations, only 2 appears feasible, as they correspond to an admissible solution space. However, only one of them is likely to occur, depending on the level of concentration of ammonia.

Then, the influence of the availability of the measurements of the uptake or production rates of the 20 amino acids is assessed. As a result, the amino acids can be classified in two groups, one with limited influence and the other with critical influence. Considering the first group, it is possible to evaluate reasonable flux distributions, even in the situation where up to 5 measurements are missing.

On the other hand, it is of interest to consider the situation where the measurements of all 20 amino acids are available (as well as, of course, standard measurements of glucose, lactate and ammonia) and to evaluate the benefits of additional measurements such as urea uptake rate, CO_2 evolution rate (CER), antibody production rate ($INF - \gamma$), Choline and Ethanolamine uptake rates. The more informative measurements appear to be CER, urea and choline uptake rates, which allow the flux intervals to be significantly reduced.

Interestingly, the resulting flux ranges can be quite narrow, thus providing a useful insight in the cell metabolism, even in the situation where some extracellular component measurements are missing and the underlying system of mass balance equations is underdetermined.

Further work will include additional experimental studies in order to built a more complete and informative data base and to support our analysis.

6 Acknowledgment

7 References

[1] KEGG: Kyoto encyclopedia of genes and genomes. online. Metabolism Map.

[2] C. Altamirano, A. Illanes, S. Becerra, J.J. Cairó, and F. Gòdia. Considerations on the lactate consumption by CHO cells in the presence of galactose. *Journal of Biotechnology*, 125:547–556, 2006.

[3] C. Altamirano, C. Paredes, A. Illanes, J.J. Cairó, and F. Gòdia. Strategies for fed-batch cultivation of t-PA producing CHO cells: substitution of glucose and glutamine and rational design of culture medium. *Journal of Biotechnology*, 110:171–179, 2004.

[4] H. P. J. Bonarius, V. Hatzimanikatis, K.P.H. Meesters, C.D.de Goojier, G. Schimd, and J. Tramper. Metabolic flux analysis of hybridoma cells in different culture media using mass balances. *Biotechnology and Bioengineering*, 50:299–318, 1996.

[5] Hendrik P. J. Bonarius, José H.M. Houtman, Cornelis D. de Gooijer, JohannesTramper, and Georg Schmid. Activity of glutamate dehydrogenase is increased in ammonia-stressed hybridoma cells. *Biotechnology and Bioengineering*, 57:447–453, 1998.

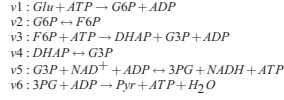[6] Hendrik P. J. Bonarius, José H.M. Houtman, Georg Schmid, Cornelis D. de Gooijer, and Johannes Tramper.

Metabolic flux analysis of hybridoma cells under oxidative and reductive stress using mas balances. *Cyto technology*, 32:97–107, 2000.

[7] Hendrik P. J. Bonarius, Georg Schmid, and Johannes Tramper. Flux analysis of underdetermined metabolic networks: the quest for the missing constraints. *TIBTECH*, 15:308–314, August 1997.

[8] Elisabeth M. A. Curling, Paul M. Hayter, Anthony J. Baines, Alan T. Bull, Keith Gull, Philip G. Strange, and Nigel Jenkins. Recombinant human interferon-γ. *Biochemical Journal*, 272:333–337, 1990.

[9] Drugbank.

[10] O. Henry, M. Perrier, and A. Kamen. Metabolic flux analysis of HEK-293 cells in perfusion cultures for the production of adenoviral vectors. *Metabolic Engineering*, 7:467–476, 2005.

[11] Wei-Shou Hu. Cell biology for process engineering. Technical report, Cellular Bioprocess Technology. University of Minnesota, 2004.

[12] H. Jakubowski. Biochemistry: Lipid structure. online, 2008.

[13] Fa-Ten Kao and Theodore T. Puck. Genetics of somatic mammalian cells, IV. properties of chinese hamster cell mutants with respect to the requirement for proline. *Genetics*, 55:513–524, 1967.

[14] Fa-Ten Kao and Theodore T. Puck. Genetics of somatic mammalian cells, VII. induction and isolation of nutritional mutants in chinese hamster cells. *Proceedings of the National Academy of Sciences of the United States of America*, 60:1275–1281, 1968.

[15] Peter H. Van Der Meide, Martin Dubbeld, Kitty Vijverberg, and Ton Kosand Huubschellekens. The purification and characterization of rat gamma interferon by use of two monoclonal antibodies. *Journal of General Virology*, 67:1059–1071, 1986.

[16] I. Nadeau, J. Sabatié, M. Koehl, M. Perrier, and A. Kamen. Human 293 cell metabolism in low glutamine-supplied culture: Interpretation of metabolic changes through metabolic flux analysis. *Metabolic Engineering*, 2:277–292, 2000.

[17] D.L. Nelson and M.M. Cox. *Lehninger, Principles of Biochemistry*. Fourth edition edition, 2005.

[18] Gregg B. Nyberg, Robert Balcarcel, Brian D. Follstad, Gregory Stephanopoulos, and Daniel I. C. Wang. Metabolism of peptide amino acids by chinese hamster ovary cells grown in a complex medium. *Biotechnology and Bioengineering*, 62:321–335, 1999.

[19] T. Pfeiffer, I. Sánchez-Valdenebro, J.C. Nuňo, F. Montero, and S. Schuster. METATOOL: for studying metabolic networks. *Bioinformatics*, 15(3):251–257, Mar 1999.

[20] A. Provost. *Metabolic Design of Dynamic Bioreaction Models*. PhD thesis, Université Catholique de Louvain, 2006.

[21] A. Provost and G. Bastin. Dynamic metabolic modelling under the balanced growth condition. *Journal of Process Control*, 14:717–728, 2004.

[22] A. Provost, G Bastin, and YJ. Schneider. From metabolic networks to minimal dynamic bioreaction models. 10th International IFAC Symposium on Computer Applications in Biotechnology, June 2007.

[23] David W. Russell. Cholesterol biosynthesis and metabolism. *Cardiovascular Drugs and Therapy*, 6:103–110, 1992.

[24] Joanne M. Savinell and Bernhard O. Palsson. Optimal selection of metabolic fluxes for in vivo measurement. I. development of mathematical methods. *Journal of Theoretical Biology*, 155:201–214, 1992.

[25] Markus Schneider, Ian W. Marison, and Urs von Stockar. The importance of ammonia in mammalian cell culture. *Journal of Biotechnology*, 46:161–185, 1996.

[26] S. Schuster, T. Dandekar, and D. A. Fell. Detection of elementary flux modes in biochemical networks: a promising tool for pathway analysis and metabolic engineering. *TIBTECH*, 17:53–60, 1999.

[27] Noboru Seoka. Directional mutation preassure and neutral molecular evolution. *Proc.Natl. Acad. Sci. USA*, 85:2653–2657, 1988.

[28] G. N. Stephanopoulos, A. A. Aristidou, and J. Nielsen. *Metabolic Engineering: Principles and Methodologies*. 1998.

[29] Gregory Stephanopoulos. Metabolic fluxes and metabolic engineering. *Metabolic Engineering*, 1:1–11, 1999.

[30] Noboru Sueoka. Correlation between base composition of deoxyribonucleic acid and amino acid composition of protein. *Proc.Natl. Acad. Sci. USA*, 47:1141–1149, 1961.

[31] Noboru Sueoka. On genetic basis of variation and heterogeneity of DNA base composition. *Proc.Natl. Acad. Sci. USA*, 48:582–592, 1962.

[32] Aljoscha Wahl, Yury Sidorenko, Michael Dauner, Yvonne Genzel, and Udo Reichl. Metabolic flux model for an anchorage-dependent MDCK cell line. *Biotechnology and Bioengineering*.

[33] Liangzhi Xie and Daniel I.C. Wang. Applications of improved stoichiometric model in medium design and fed-batch cultivation of animal cells in bioreactor. *Cytotechnology*, 15:17–29, 1994.

[34] Craig Zupke and Gregory Stephanopoulos. Intracellular flux analysis in hybridomas using mass balances and in vitro ^{13}C NMR. *Biotechnology and Bioengineering*, 45:292–303, 1995.

Figure 4: Reduction Percentage of Flux Intervals by adding Hypothetical Measurements

A Complex Metabolic Network

Glycolysis

$$v1 : Glu + ATP \rightarrow G6P + ADP$$
$$v2 : G6P \leftrightarrow F6P$$
$$v3 : F6P + ATP \rightarrow DHAP + G3P + ADP$$
$$v4 : DHAP \leftrightarrow G3P$$
$$v5 : G3P + NAD^+ + ADP \leftrightarrow 3PG + NADH + ATP$$
$$v6 : 3PG + ADP \rightarrow Pyr + ATP + H_2O$$

Tricarboxylic acid cycle

$$v7 : Pyr + NAD^+ + CoASH \rightarrow AcCoA + CO_2 + NADH$$
$$v8 : AcCoA + Oxal + H_2O \rightarrow Cit + CoASH$$
$$v9 : Cit + NAD(P)^+ \rightarrow \alpha KG + CO_2 + NAD(P)H$$
$$v10 : \alpha KG + CoASH + NAD^+ \rightarrow SucCoA + CO_2 + NADH$$
$$v11 : SucCoA + GDP + P_i \leftrightarrow Succ + GTP + CoASH$$
$$v12 : Succ + FAD \leftrightarrow Fum + FADH_2$$
$$v13 : Fum + H_2O \leftrightarrow Mal$$
$$v14 : Mal + NAD^+ \leftrightarrow Oxal + NADH$$

Pyruvate Fates

$$v15 : Pyr + NADH \leftrightarrow Lact + NAD^+$$
$$v16 : Pyr + Glu \leftrightarrow Ala + \alpha KG$$

Pentose Phosphate Pathway

$$v17 : G6P + 2NADP^+ + H_2O \rightarrow Rbl5P + 2NADPH + CO_2$$
$$v18 : Rbl5P \leftrightarrow R5P$$
$$v19 : Rbl5P \leftrightarrow X5P$$
$$v20 : X5P \leftrightarrow R5P$$
$$v21 : X5P + R5P \leftrightarrow S7P + G3P$$
$$v22 : S7P + G3P \leftrightarrow F6P + E4P$$
$$v23 : X5P + E4P \leftrightarrow G3P + F6P$$

Anaplerotic Reaction

$$v24 : Mal + NAD(P)^+ \xleftrightarrow{} Pyr + HCO_3^- + NAD(P)H$$

Amino Acid Metabolism

$$v25 : Glu + H_2O + NAD(P)^+ \xleftrightarrow{} \alpha KG + NH_4^+ + NAD(P)H$$
$$v26 : Oxal + Glu \xleftrightarrow{} Asp + \alpha KG$$
$$v27 : Gln + H_2O \rightarrow Glu + NH_4^+$$
$$v28 : Thr + NAD^+ + CoASH \rightarrow Gly + NADH + AcCoA$$
$$v29 : 3PG + Glu + NAD^+ + H_2O \rightarrow Ser + \alpha KG + NADH$$
$$v30 : Ser \leftrightarrow Gly + H_2O$$
$$v31 : Gly + NAD^+ \rightarrow CO_2 + NH_4^+ + NADH$$
$$v32 : Ser \rightarrow Pyr + NH_4^+$$
$$v33 : Thr \rightarrow \alpha Kb + H_2O + NH_4^+$$
$$v34 : \alpha Kb + CoASH + NAD^+ \rightarrow PropCoA + NADH + CO_2$$
$$v35 : PropCoA + HCO_3^- + ATP \rightarrow SucCoA + ADP + P_i$$
$$v36 : Trp \rightarrow Ala + 2CO_2 + \alpha Ka$$
$$v37 : Lys + 2\alpha KG + 2NADP^+ + NAD^+ + FAD^+ + 3H_2O \rightarrow \alpha Ka + 2Glu + 2NADPH + NADH + FADH_2$$
$$v38 : \alpha Ka + CoASH + 2NAD^+ + H_2O \rightarrow AcetoAcCoA + 2NADH + 2CO_2$$
$$v39 : AcetoAcCoA + CoASH \rightarrow 2AcCoA$$
$$v40 : Val + \alpha KG + CoASH + 3NAD^+ + FAD^+ + 2H_2O \rightarrow PropCoA + Glu + 2CO_2 + 3NADH + FADH_2$$
$$v41 : Ile + \alpha KG + 2CoASH + 2NAD^+ + FAD^+ + H_2O \rightarrow AcCoA + PropCoA + Glu + CO_2 + 2NADH + FADH_2$$
$$v42 : Leu + \alpha KG + CoASH + NAD^+ + HCO_3^- + ATP + FAD^+ + H_2O \rightarrow AcCoA + AcetoAc + Glu + CO_2 + NADH + ADP + FADH_2$$
$$v43 : AcetoAc + SucCoA \rightarrow AcetoAcCoA + Succ$$
$$v44 : Phe + NADH \rightarrow Tyr + NAD^+ + H_2O$$
$$v45 : Tyr + \alpha KG + H_2O \rightarrow Fum + AcetoAc + Glu + CO_2$$
$$v46 : Met + Ser + ATP + 2H_2O \rightarrow Cys + \alpha Kb + NH_4^+ + AMP$$
$$v47 : Cys + H_2O \rightarrow Pyr + NH_4^+$$
$$v48 : Asn + H_2O \rightarrow Asp + NH_4^+$$
$$v49 : Arg + H_2O \rightarrow Orn + Urea$$
$$v50 : Orn + \alpha KG \leftrightarrow Glu\gamma SA + Glu$$
$$v51 : Pro \rightarrow Glu\gamma SA + H_2O$$
$$v52 : Glu\gamma SA + NAD(P)^+ \rightarrow Glu + NAD(P)H$$
$$v53 : His + 2H_2O \rightarrow Glu + NH_4^+$$

Urea Cycle

$$v54 : Orn + CarbP \rightarrow Cln$$
$$v55 : Cln + Asp + ATP \rightarrow ArgSucc + AMP$$
$$v56 : ArgSucc \rightarrow Arg + Fum$$

Proteine Synthesis

$$v57 : 0.023His + 0.053Ile + 0.091Leu + 0.059Lys + 0.023Met + 0.039Phe + 0.059Thr + 0.014Trp$$
$$+ 0.066Val + 0.051Arg + 0.019Cys + 0.042Gln + 0.072Gly + 0.052Pro + 0.032Tyr + 0.78Ala$$
$$+ 0.043Asn + 0.053Asp + 0.063Glu + 0.068Ser + ATP + 3GTP \rightarrow Protein + AMP + Pp_i + 3GDP + 3P_i$$

INF-γ Synthesis

$$INF - \gamma : 0.0137His + 0.0479Ile + 0.0685Leu + 0.1370Lys + 0.0274Met + 0.0685Phe + 0.0342Thr$$
$$+ 0.0068Trp + 0.0548Val + 0.0548Arg + 0.0137Cys + 0.0616Gln + 0.0342Gly + 0.0137Pro + 0.0342Tyr$$
$$+ 0.0548Ala + 0.0685Asn + 0.0685Asp + 0.0616Glu + 0.0753Ser + ATP + 3GTP \rightarrow INF - \gamma + AMP + Pp_i + 3GDP + 3P_i$$

Nucleotide Synthesis

$$v58 : R5P + ATP \rightarrow PRPP + AMP$$
$$v59 : PRPP + 2Gln + Gly + Asp + 4ATP + CO_2 \rightarrow IMP + 2Glu + Fum + 4ADP + 2H_2O$$
$$v60 : IMP + Asp + ATP + GTP \rightarrow ADP_{RN} + Fum + ADP + GDP$$
$$v61 : ADP_{RN} + ATP \leftrightarrow ATP_{RN} + ADP$$
$$v62 : IMP + Gln + 2ATP + NAD^+ + 2H_2O \rightarrow GDP_{RN} + Glu + ADP + AMP + NADH$$
$$v63 : GDP_{RN} + ATP \leftrightarrow GTP_{RN} + ADP$$
$$v64 : HCO_3^- + NH_4^+ + 2ATP \rightarrow CarbP + ADP$$
$$v65 : CarbP + PRPP + Asp + ATP + NAD^+ \rightarrow UDP_{RN} + ADP + NADH + CO_2 + H_2O$$
$$v66 : UDP_{RN} + ATP \leftrightarrow UTP_{RN} + ADP$$
$$v67 : UTP_{RN} + Gln + ATP \rightarrow CTP_{RN} + Glu + ADP$$
$$v68 : CTP_{RN} + ADP \leftrightarrow CDP_{RN} + ATP$$
$$v69 : 0.285(ATP_{RN} + UTP_{RN}) + 0.215(GTP_{RN} + CTP_{RN}) \rightarrow RNA$$
$$v70 : ADP_{RN} + ATP \rightarrow dATP + ADP + H_2O$$
$$v71 : GDP_{RN} + ATP \rightarrow dGTP + ADP + H_2O$$
$$v72 : CDP_{RN} + ATP \rightarrow dCTP + ADP + H_2O$$
$$v73 : UDP_{RN} + ATP \rightarrow dUTP + ADP + H_2O$$
$$v74 : dUTP \rightarrow dTTP$$
$$v75 : 0.285(dATP + dTTP) + 0.215(dGTP + dCTP) \rightarrow DNA$$

Lipid Synthesis
Fatty Acids

$$v76 : AcCoA + HCO_3^- + ATP \rightarrow MalCoA + ADP$$
$$v77 : 7MalCoA + AcCoA + 14NADPH \rightarrow Palmitate + 7CO_2 + 8CoASH + 14NADP^+ + 6H_20$$
$$v78 : Palmitate + CoASH + ATP \rightarrow PalmCoA + AMP$$
$$v79 : PalmCoA + MalCoA + 2NADPH \rightarrow Stearate + 2NADP^+ + CO_2 + CoASH$$
$$v80 : Stearate + CoASH + ATP \rightarrow SteCoA + AMP$$
$$v81 : SteCoA + NADH \rightarrow Oleate + NAD^+ + H_2O + CoASH$$
$$v82 : Oleate + CoASH + ATP \rightarrow OleCoA + AMP$$

Glycerophospholipids

$$v83 : DHAP + NADH \rightarrow Glyc3P + NAD^+$$
$$v84 : PalmCoA + OleCoA + Glyc3P \rightarrow PA$$
$$v85 : SteCoA + OleCoA + Glyc3P \rightarrow PA$$
$$v86 : PA + H_2O \rightarrow 1,2DG$$
$$v87 : Choline + 1,2DG + ATP + CTP \rightarrow PC + ADP + CMP$$
$$v88 : Ethanolamine + 1,2DG + ATP + CTP \rightarrow PE + ADP + CMP$$
$$v89 : PE + Ser \rightarrow PS + Ethanolamine$$
$$v90 : PS \rightarrow PE + CO_2$$

Sphingolipids

$$v91 : PalmCoA + Ser + NADPH \rightarrow Sphinganine + NADP^+ + CoASH + CO_2$$
$$v92 : Sphinganine + PalmCoA \rightarrow Ceramide + CoASH$$
$$v93 : Sphinganine + SteCoA \rightarrow Ceramide + CoASH$$
$$v94 : Sphinganine + OleCoA \rightarrow Ceramide + CoASH$$
$$v95 : Ceramide + PC \rightarrow SM + 1,2DG$$
$$v96 : Ceramide + PE \rightarrow SM + 1,2DG$$

Cholesterol Synthesis

$$v97 : 3AcCoA + 2NADPH \rightarrow Mevalonate + 3CoASH + 2NAD^+$$
$$v98 : Mevalonate + 3ATP \rightarrow IsopentenylpyroP + 2ADP + CO_2$$
$$v99 : IsopentenylpyroP \leftrightarrow DimethylallylpyroP$$
$$v100 : IsopentenylpyroP + DimethylallylpyroP \rightarrow GeranylpyroP$$
$$v101 : IsopentenylpyroP + GeranylpyroP \rightarrow FarnesylpyroP$$
$$v102 : 2FarnesylpyroP + 2NADPH \rightarrow Cholesterol + 2NADP^+ + H_2O$$

Membrane Lipid

$$v103 : 0.5PC + 0.2PE + 0.075PS + 0.075SM + 0.15Cholesterol \rightarrow MembraneLipid$$

Transport Reactions

$$v104 : Gln_{ext} \rightarrow Gln$$
$$v105 : Ala \rightarrow Ala_{ext}$$
$$v106 : Gly \rightarrow Gly_{ext}$$
$$v107 : Ser_{ext} \rightarrow Ser$$
$$v108 : Glu_{ext} \rightarrow Glu$$
$$v109 : Asn_{ext} \rightarrow Asn$$
$$v110 : Asp_{ext} \rightarrow Asp$$
$$v111 : Cys_{ext} \rightarrow Cys$$
$$v112 : Arg_{ext} \rightarrow Arg$$
$$v113 : Pro_{ext} \rightarrow Pro$$
$$v114 : Tyr_{ext} \rightarrow Tyr$$
$$v115 : Etn_{ext} \rightarrow Etn$$

By Products

$$v116 : CO_2 \rightarrow CO_{2,ext}$$
$$v117 : NH_4^+ \rightarrow NH_{4,ext}^+$$